Aharonov-Bohm effect on the bound states of an electron inside an annular cylindrical box

D. Kouznetsov
Hopelchen 353 L13, Colonia Torres de Padierna, 14200 México, D.F. Mexico

E. Ley-Koo and G. Villa-Torres
Instituto de Física, Universidad Nacional Autónoma de México
Apartado postal 20-364, 01000 México, D.F., Mexico

Recibido el 16 de marzo de 1999; aceptado el 1 de julio de 1999

We solve the Schröedinger equation for an electron inside an annular cylindrical box in two situations: *i)* in the absence of any fields, and *ii)* in the presence of a uniform, axial magnetic induction field confined and centered in the perforation. The Aharonov-Bohm effect on the bound states of the electron is exhibited through the analysis of the dependence of the energy eigenvalues and eigenfunctions on the enclosed magnetic flux. The results of this study serve to illustrate the roles of the magnetic vector potential and the gauge transformations in quantum mechanics.

Keywords: Magnetic vector potential in quantum mechanics

Se resuelve la ecuación de Schröedinger para un electrón en el interior de una caja anular cilíndrica en dos situaciones; *i)* en ausencia de cualquier campo, y *ii)* en presencia de un campo de inducción magnética axial y uniforme confinado y centrado en la perforación. Se exhibe el efecto Aharonov-Bohm sobre los estados ligados del electrón a través del análisis de la dependencia de los eigenvalores de la energía y las eigenfunciones con respecto al flujo magnético encerrado. Los resultados de este estudio sirven para ilustrar los papeles del potencial vectorial magnético y las transformaciones de norma en mecánica cuántica.

Descriptores: Potencial vectorial magnético en mecánica cuántica

PACS: 03.65

1. Introduction

It is almost forty years since Aharonov and Bohm analyzed the significance of the electromagnetic vector potential in quantum theory, and suggested an experiment to test for the effect of the potential in regions where there are no magnetic fields [1]. They predicted that the fringe pattern in an electron interference experiment should be shifted by altering the amount of magnetic flux passing between two beams, even though the beams themselves pass only through field-free regions. Specifically, a shift of ν fringes is associated with an enclosed flux of $\nu hc/e$, where the natural unit of flux or fluxon, $hc/e = 4.135 \times 10^{-7}$ gauss $\cdot$ cm^2, is determined by the Planck constant h, the velocity of light c, and the electron's electric charge e. Within a year, Chambers performed such an experiment reporting the expected shifts of an electron interference pattern by the corresponding magnetic fluxes, including situations in which the pattern appears unchanged due to their association with magnetic fluxes of an integer number of fluxons [2].

It is also twenty years since two didactic articles on related topics were published [3, 4]. In the first one, Konopinski discussed the explicit physical meaning and direct measurability of the electromagnetic vector potential in the classical context. And in the second one, Kobe deduced Maxwell's equations from the gauge invariance of quantum mechanics. Konopinski's book on electromagnetism [5] and Sakurai's books on quantum mechanics [6, 7] contain more detailed treatments of these topics.

Bound state versions of the Aharonov-Bohm effect have also been discussed in the literature [8, 9]. In the specialized book of Peshkin and Tonomura [8], the first author illustrated the effect for the charged rotator in a plane, and pointed out that there are no important changes if the motion is allowed to be three-dimensional inside a torus. In Ballentine's book [9] the charged particle confined to the interior of a torus of rectangular cross-section is also used to recognize that the energy of the stationary states must depend on the magnetic flux in the perforation. In both references the respective authors considered that the detailed quantitative analysis of the problem was not necessary for their purposes.

This paper presents a bound state version of the Aharonov-Bohm effect through the study of the energy spectra and eigenfunctions of an electron inside an annular cylindrical box in two comparative situations: *i)* in the absence of any fields, and *ii)* in the presence of a uniform, axial magnetic induction field confined and centered in the perforation with its associated magnetic vector potential in the interior of the box. In Sect. 2, the reference problem of situation *i)* is formulated and solved for the electron inside a box defined in cylindrical coordinates ($a \leq \rho \leq b$, φ, $0 \leq z \leq L$). Section 3 contains the formulation and solution of the Aharonov-

Bohm problem involving a magnetic induction field $\vec{B} = \hat{k}B$ confined in $(0 < \rho < \rho_0 \leq a,\ \varphi,\ z)$ and the magnetic vector potential $\vec{A} = \hat{\varphi}B\rho_0^2/2\rho$ inside the box. Section 4 presents illustrative numerical and graphical results of the solutions for the energy eigenvalues and eigenfunctions as the magnetic flux enclosed inside the perforation, $\nu = (B\pi\rho_0^2)/(hc/e)$, is changed. Section 5 contains a discussion of the Aharonov-Bohm effect on the bound states with emphasis on the symmetry and periodicity of the energy spectra as functions of ν, including the degeneraces for integer and half-integer values.

2. The electron inside an annular cylindrical box

The Schröedinger equation for the electron inside an annular cylindrical box in cylindrical coordinates,

$$-\frac{\hbar^2}{2m_e}\left[\frac{1}{\rho}\frac{\partial}{\partial\rho}\rho\frac{\partial}{\partial\rho} + \frac{1}{\rho^2}\frac{\partial^2}{\partial\varphi^2} + \frac{\partial^2}{\partial z^2}\right]\psi(\rho,\varphi,z) = E\psi(\rho,\varphi,z), \quad (1)$$

must be solved subject to the boundary condition that the wavefunction vanishes at the positions of the walls of the box:

$$\psi(\rho = a,\varphi,z) = \psi(\rho = b,\varphi,z) = 0, \quad (2a)$$

$$\psi(\rho,\varphi,z) = \psi(\rho,\varphi + 2\pi,z), \quad (2b)$$

$$\psi(\rho,\varphi,z = 0) = \psi(\rho,\varphi,z = L) = 0. \quad (2c)$$

Equation (1) is known to admit the separable solution

$$\psi(\rho,\varphi,z) = R(\rho)\Phi(\varphi)Z(z), \quad (3)$$

in which the respective factors satisfy the ordinary differential equations

$$\frac{\mathrm{d}^2Z(z)}{\mathrm{d}z^2} = -k_L^2 Z(z), \quad (4a)$$

$$\frac{\mathrm{d}^2\Phi(\varphi)}{\mathrm{d}\varphi^2} = -m^2\Phi(\varphi), \quad (4b)$$

$$\left[\frac{1}{\rho}\frac{\mathrm{d}}{\mathrm{d}\rho}\rho\frac{\mathrm{d}}{\mathrm{d}\rho} - \frac{m^2}{\rho^2}\right]R(\rho) = -k_T^2 R(\rho), \quad (4c)$$

and the energy eigenvalue is the sum of the transverse and longitudinal contributions,

$$E = \frac{\hbar^2}{2m_e}(k_T^2 + k_L^2). \quad (5)$$

The solutions of Eq. (4a) subject to the boundary conditions of Eq. (2c) are

$$Z(z) = \sqrt{\frac{2}{L}}\sin\frac{n\pi z}{L}, \qquad n = 1,2,3,\ldots \quad (6)$$

The solutions of Eq. (4b) are the eigenfuctions of the z-component of the orbital angular momentum,

$$\Phi(\varphi) = \frac{e^{im\varphi}}{\sqrt{2\pi}}, \qquad m = 0,\pm1,\pm2,\ldots \quad (7)$$

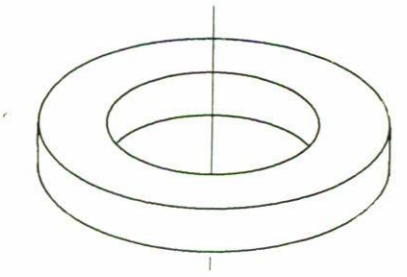

FIGURE 1. Annular cylindrical box with inner radius a, outer radius b and height L. A uniform axial magnetic induction field is applied and centered in the perforation.

Equation (4c) is recognized as the Bessel equation and its general solution is the linear combination of the ordinary Bessel function and the Neumann function [10],

$$R(\rho) = \mathcal{A}_m J_m(k_{\mathrm{T}}\,\rho) + \mathcal{B}_m Y_m(k_{\mathrm{T}}\,\rho), \quad (8)$$

since m is an integer, Eq. (7). The boundary conditions of Eqs. (2a) on this solution are expressed by

$$\mathcal{A}_m J_m(k_T a) + \mathcal{B}_m Y_m(k_T a) = 0, \quad (9a)$$

$$\mathcal{A}_m J_m(k_T b) + \mathcal{B}_m Y_m(k_T b) = 0. \quad (9b)$$

This is a set of two algebraic homogeneous linear equations for the unknown coefficients $\mathcal{A}_m$ and $\mathcal{B}_m$, which admits nontrivial zero solutions only if its determinant vanishes, *i.e.*,

$$J_m(k_T a)Y_m(k_T b) - J_m(k_T b)Y_m(k_T a) = 0. \quad (10)$$

This transcendental equation has to be solved numerically to obtain the transverse wave number k_{T}. The task is accomplished by using numerical recipes in C [11]. Let $k_{\mathrm{T}}a = x_{ms}$ be the successive solutions $s = 1,2,3,\ldots$, for given values of a and b. The energy eigenvalues of Eq. (5) with the explicit values of the wavenumbers from Eqs. (5) and (10) are given by

$$E_{msn} = \frac{\hbar^2}{2m_e}\left(\frac{x_{ms}^2}{a^2} + \frac{n^2\pi^2}{L^2}\right), \quad (11)$$

in terms of the azimuthal m, radial s and axial n quantum numbers.

The ratio of the coefficients $\mathcal{A}_m$ and $\mathcal{B}_m$ follows from Eq. (9a) or Eq. (9b), and it allows to write the normalized radial eigenfuction, Eq. (8), as

$$R_{ms}(\rho) = \frac{1}{\sqrt{\mathcal{N}_{ms}}}\left[Y_m\left(\frac{x_{ms}b}{a}\right)J_m\left(\frac{x_{ms}\rho}{a}\right) - J_m\left(\frac{x_{ms}b}{a}\right)Y_m\left(\frac{x_{ms}\rho}{a}\right)\right], \quad (12)$$

where the normalization constant is

$$\mathcal{N}_{ms} = \int_a^b\left[Y_m\left(\frac{x_{ms}b}{a}\right)J_m\left(\frac{x_{ms}\rho}{a}\right) - J_m\left(\frac{x_{ms}b}{a}\right)Y_m\left(\frac{x_{ms}\rho}{a}\right)\right]^2\rho\,\mathrm{d}\rho. \quad (13)$$

The problem of this section has also been studied in the specialized research literature [12].

3. Aharonov-Bohm effect on the bound states of the electron

In this section we formulate and solve the problem with the magnetic induction field confined in the perforation of the annular box and its associated magnetic vector potential inside the box. The Hamiltonian for the system is given by the minimal coupling prescription

$$\hat{H} = \frac{(\hat{\vec{p}} + \frac{e}{c}\vec{A})^2}{2m_e}, \tag{14}$$

in which $\hat{\vec{p}} = -i\hbar\nabla$ is the "conjugate" momentum and the second term is the negative of the "potential momentum" of the electron in the magnetic vector potential [3, 5]. Then the Schödinger equation can be written as

$$\left\{ -\frac{\hbar^2}{2m_e}\frac{1}{\rho}\frac{\partial}{\partial\rho}\rho\frac{\partial}{\partial\rho} + \frac{\left(\ell_z + \frac{eB\rho_o^2}{2c}\right)^2}{2m_e\rho^2} - \frac{\hbar^2}{2m_e}\frac{\partial^2}{\partial z^2}\right\}\psi(\rho,\varphi,z) = E\psi(\rho,\varphi,z). \tag{15}$$

Comparison of Eqs. (1) and (15) shows that they share the same radial and longitudinal contributions to the kinetic energy, and their difference resides in the extra term arising from the magnetic vector potential and added to the z-component of the angular momentum

$$\frac{eB\pi\rho_0^2}{2\pi c} = \hbar\nu, \tag{16}$$

where ν is the magnitude of the magnetic flux in the perforation in the units hc/e. Equation (15) also admits a separable solution of the same form as Eq. (3). Equations (4a) and (6) for the longitudinal eigenfunctions continue to be valid. The eigenfunctions of the z-component of the angular momentum of Eq. (7) are also eigenfunctions of the angular operator of Eq. (15):

$$(\hat{\ell}_z + \hbar\nu)\Phi_m(\varphi) = \hbar(m+\nu)\Phi_m(\varphi). \tag{17}$$

Then the radial part of Eq. (15) becomes

$$\left[\frac{1}{\rho}\frac{\mathrm{d}}{\mathrm{d}\rho}\rho\frac{\mathrm{d}}{\mathrm{d}\rho} - \frac{(m+\nu)^2}{\rho^2}\right]R(\rho) = -k_{\mathrm{T}}^2\,R(\rho). \tag{18}$$

Comparison of the radial Eqs. (4c) and (18) shows that they are of the same type with the difference in their parameters,

$$m \longrightarrow M = m + \nu. \tag{19}$$

While the values of m are restricted to be integers, Eq. (7), the values of M can vary continuously following the corresponding variations of the magnetic flux ν. The solution of the radial Eq. (18) follows the same steps of Eqs. (8)–(13) with the substitution of m by M of Eq. (19).

It is also important to recognize that while the eigenstates of Eq. (4c) given by Eq. (12) are doubly degenerate for $m = \pm1, \pm2, \ldots$, such a degeneracy is removed when there is magnetic flux in the perforation, since the corresponding parameters from Eq. (19), $M = |m| + \nu$ and $M = -|m| + \nu$ are different. On the other hand, starting from given values of m and ν there are an infinite number of combinations of successive values of such parameters,

$$M = m + \nu = (m - N) + (\nu + N), \qquad N = 0, \pm1, \pm2, \pm3, \ldots \tag{20}$$

consistent with the same value of M. The different states for the different magnetic fluxes have the same energies, which translates into a periodic repetition of the energy spectrum as the magnetic flux increases by one unit. In particular, the energy spectra for $\nu = 1, 2, 3, \ldots$ are the same as for $\nu = 0$ including ground states with $m = -1, -2, -3, \ldots$ and excited doubly degenerate states with $m = 0$ and -2, 1 and -3, 2 and $-4, \ldots$; -1 and -3, 0 and -4, 1 and $-5, \ldots$; -2 and -4, -1 and -5, 0 and $-6, \ldots$; $\ldots$; respectively. By considering the interval $0 < \nu < 1$, and the states with $m = |m|$ and $-|m| - 1$, we identify the common value of

$$M = |m| + \nu \quad \text{and} \quad -M = -(|m| + 1) + (1 - \nu), \tag{21}$$

leading to the same values of the transverse energies. Notice that the states involved are neighbour states in the angular momentum quantum number and have the same energy for complementary values of the magnetic flux, ν and $1 - \nu$. The net result is that the energy of the $|m|$-state increases monotonically as ν changes between 0 and 1, while the energy of the $(-|m| - 1)$-state also increases monotonically in the same way as $1 - \nu$ changes between 0 and 1. In other words, the latter decreases monotonically as ν changes between 0 and 1. For $\nu = 0.5$ both states have the same energy for the common value of the magnetic flux, producing another situation of double degeneracy. The respective energy curves are symmetric relative to the line $\nu = 0.5$.

4. Illustrative numerical and graphical results

In this section we present some quantitative results illustrating the solutions of the eigenvalue problems formulated in Sects. 2 and 3. The emphasis is on the transverse contribution to the energy eigenvalues and the associated radial eigenfunctions. The numerical results are contained in tables and figures for both cases $\nu = 0$ and $\nu \neq 0$ together.

Figure 2 is a graph of the determinant appearing in Eq. (10)

$$D_M(x) = J_M(x)Y_M\left(\frac{bx}{a}\right) - Y_M(x)J_M\left(\frac{bx}{a}\right), \tag{22}$$

as a function of $x = k_{\mathrm{T}}a$ for different values of the parameter M, Eq. (19), and for the specific case of $b = 2a$. Its zeros x_{M_s}, determined through the corresponding program of [11], are contained in Table I.

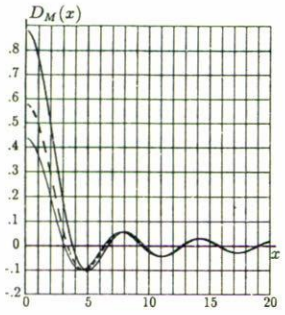

FIGURE 2. Graph of the determinant $D_M(x)$ of Eq. (22) for $M = 0$ (thin line), 1.9 (dashed line) and 3.14 (solid line), and $b = 2a$. Its zeros determine the transverse wave number and the energy eigenvalues according to Eqs. (10) and (11).

TABLE I. Zeros of Eq. (22) x_{Ms} for different values of M and s, and $b = 2a$. Their squares correspond to the transverse energy eigenvalues, Eq. (11).

M \ s	1	2	3	4
0.0	3.12303	6.27344	9.41821	12.56142
0.2	3.12601	6.27500	9.41926	12.56221
0.4	3.13492	6.27968	9.42241	12.56459
0.6	3.14972	6.28747	9.42767	12.56855
0.8	3.17031	6.29837	9.43502	12.57408
1.0	3.19658	6.31235	9.44447	12.58120
1.2	3.22836	6.32940	9.45600	12.58990
1.4	3.26550	6.34950	9.46961	12.60017
1.6	3.30778	6.37261	9.48530	12.61201
1.8	3.35500	6.39871	9.50305	12.62541
2.0	3.40692	6.42777	9.52285	12.64038
2.2	3.46332	6.45974	9.54470	12.65691
2.4	3.52396	6.49458	9.56857	12.67499
2.6	3.58859	6.53226	9.59447	12.69461
2.8	3.65697	6.57272	9.62236	12.71578
3.0	3.72887	6.61592	9.65225	12.73848
3.2	3.80406	6.66181	9.68410	12.76271
3.4	3.88231	6.71033	9.71791	12.78846
3.6	3.96342	6.76144	9.75365	12.81572
3.8	4.04716	6.81507	9.79131	12.84449
4.0	4.13337	6.87116	9.83086	12.87474
4.2	4.22183	6.92967	9.87230	12.90649
4.4	4.31239	6.99054	9.91559	12.93971
4.6	4.40488	7.05369	9.96072	12.97440
4.8	4.49914	7.11908	10.00766	13.01055
5.0	4.59502	7.18665	10.05639	13.04814

Figure 3 shows the energy levels of the states with lowest angular excitations $m = 0, \pm1, \pm2, \ldots$ and no radial excitation $s = 1$, as functions of the magnetic flux ν in the perforation. According to Eq. (11) and its extension for the case $\nu \neq 0$, the energy levels correspond to the squares of the zeros of Table I, x_{Ms}^2, in units of $\hbar^2/(2m_e a^2)$. The reader may appreciate the periodicity of the energy spectra as ν changes by one unit, the double degeneracy of the states for integer and half-integer values of ν, and the symmetry of the energy curves within each unit interval of ν under reflection with respect to the line with the corresponding half-integer value of ν.

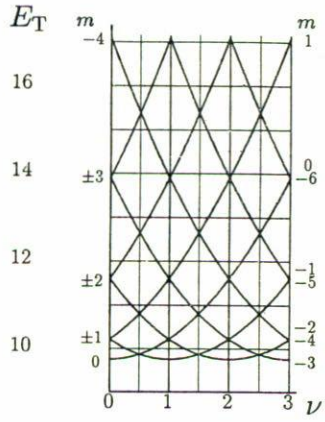

FIGURE 3. Transverse energy eigenvalues E_T in units $\hbar^2/2m_e a^2$ as functions of the magnetic flux ν in units ch/e, for states with the lowest angular excitations $m = 0, \pm1, \pm2, \ldots$ and no radial excitation $s = 1$, and $b = 2a$.

TABLA II. Transverse wavenumbers $k_T = x_{Ms}/a$ and coefficients of normalized radial eigenfunction $\mathcal{A}_{Ms}$ and $\mathcal{B}_{Ms}$, Eqs. (8) and (12), for different values of M and s, and $b = 2a$.

M	s	x_{Ms}	$\mathcal{A}_M$	$\mathcal{B}_M$
0	1	3.123039	1.18538	1.37124
	2	6.273439	1.73003	1.89366
	3	9.418211	2.14125	2.29878
	4	12.561424	2.48549	2.64229
	5	15.704000	2.78759	2.94595
	6	18.846249	3.06003	3.22109
1.9	1	3.380384	−1.80494	0.17472
	2	6.412872	−2.48722	−0.60375
	3	9.512694	−2.93332	−1.11832
	4	12.632701	−3.29758	−1.50910
	5	15.761176	−3.61801	−1.83150
	6	18.893965	−3.90917	−2.11052
3.14	1	3.781170	−1.42795	−1.10560
	2	6.647763	−0.21997	−2.55717
	3	9.674336	0.79896	−3.03178
	4	12.755284	1.54066	−3.28064
	5	15.859745	2.11991	−3.45593
	6	18.976334	2.59959	−3.60214

Table II presents a sample of the coefficients $\mathcal{A}_M$ and $\mathcal{B}_M$ of the radial function of Eq. (8) and its extensions for $\nu \neq 0$, normalized according to Eqs. (12) and (13).

5. Discussion

The comparative analysis of the formulations and results of the problems of Sects. 2 and 3 serves to exhibit the effects of the magnetic vector potential on the energy eigenvalues and eigenstates of the electron inside the annular box, in which there is no magnetic force field. From the analysis at the end of Sect. 3 and the results of Sect. 4 some general statements about the Aharonov-Bohm effect on the electron's energy eigenvalues, as functions of the magnitude of the magnetic flux in the perforation, can be made. These statements are valid for any chosen values of the radial and longitudinal quantum numbers s and n.

1) The energy eigenvalues of the states with $m = 0, 1, 2, \ldots$ increase monotonically with ν, in such a way that

$$E_m(\nu + 1) = E_{m+1}(\nu), \tag{23a}$$

and the corresponding iterative extension

$$E_m(\nu + N) = E_{m+N}(\nu) \quad \text{for} \quad N = 1, 2, 3, \ldots \tag{23b}$$

2) The energy eigenvalues with $m = -1, -2, \ldots$ decrease monotonically at first, in such a way that they follow Eqs. (23a) and (23b) with the negative values of m, until the magnetic flux takes the values $\nu = -m$. From this value on, each one increases following the same Eqs. (23a) and (23b).

3) Equations (23a) and (23b) describe the periodic nature of the energy spectra as functions of the magnetic flux ν with period one.

A. For $\nu = 0$, the ground state $m = 0$ is nondegenerate and the excited states $m = \pm 1, \pm 2, \ldots$ are doubly degenerate. For $\nu = N$, the ground state is the $m = -N$ state and the doubly degenerate excited states correspond to $m = -N - K$ and $-N + K$, with $K = 1, 2, 3, \ldots$

B. For $\nu = 0.5$ the ground and excited states are all doubly degenerate corresponding to $m = 0$ and -1, and K and $-K - 1$, with $K = 1, 2, 3, \ldots$ respectively. For $\nu = N + 0.5$, the corresponding states have $m = -N$ and $-N - 1$, and $-N + K$ and $-N - 1 - K$.

C. The symmetry of the energy curves in the interval $0 \leq \nu \leq 1$ with respect to reflection in the line $\nu = 0.5$, is repeated in each interval $N \leq \nu \leq N + 1$ with respect to reflection in the line $\nu = N + 0.5$.

It is also instructive to evaluate the energy of the radiative transitions between two transverse states, which follows from the counterpart of Eq. (11) with the substitution $m \to M$ and for the same longitudinal quantum number $n' = n$ with the result

$$\Delta E(Msn \to M's'n) = \frac{\hbar^2}{2m_e a^2}\left(x^2_{Ms} - x^2_{M's'}\right) \quad \text{for} \quad m' = m \pm 1. \tag{24}$$

The selection rule for the angular momentum quantum number m is the usual standard one for electric dipole transitions [6, 7]. The size of the annular box determines the region of the spectrum for the corresponding radiations. In practice, they could be detected in microscopic conducting rings [13], mesoscopic semiconducting devices [14] and nanometric quantum dots [15], corresponding to microwave, far infrared and near infrared radiations, respectively. While the enclosed magnetic flux is not always quantized, the Aharonov-Bohm effect should open new possibilities in the construction of ultra-sensitive detectors.

As a conclusion of this discussion it is also enlightening to compare the Aharonov-Bohm effect in the standard version of the interference pattern of the electrons and of the electron bound-states version of this paper. The common feature of both versions is their periodicity with period $\nu = 1$, of the interference pattern and of the energy spectrum, respectively. Both versions are solutions of the same physical problem described by the common Schröedinger equation, and their difference consists in their correspondence with scattering states and bound states, respectively.

1. Y. Aharonov and D. Bohm, *Phys. Rev.* **115** (1959) 485.
2. R.G. Chambers, *Phys. Rev. Lett.* **5** (1960) 3.
3. E.J. Konopinski, *Am. J. Phys.* **46** (1978) 499.
4. D.H. Kobe, *Am. J. Phys.* **46** (1978) 342.
5. E.J. Konopinski, *Electromagnetic Fields and Relativistic Particles*, (McGraw-Hill, New York, 1981) p. 158.
6. J.J. Sakurai, *Advanced Quantum Mechanics*, (Addison-Wesley, Reading MA, 1967) p. 11, p. 14, and p. 41.
7. J. J. Sakurai and S.F. Tuan, *Modern Quantum Mechanics*, (Addison-Wesley, Reading, MA, 1994) p. 130 and p. 338.
8. M. Peshkin and A. Tonomura, *The Aharonov-Bohm Effect*, (Springer-Verlag, Berlin Heidelberg, 1989) p. 10.
9. L. Ballentine, *Quantum Mechanics*, (Prentice Hall, Englewood Cliff, N.J., 1990) p. 222.
10. M. Abramowitz and I. Stegun, *Handbook of Mathematical Functions*, (Dover, New York, 1965) Chapt. 9.
11. W.H. Press, S.A. Teukolsky, W.T. Vitterling, and B.P. Flannery, *Numerical Recipes in C. The Art of Scientific Computing*, (U.P. Cambridge New York, U.S.A., 1992) Chapt. 9.
12. M. Kumagai and T. Ohno, *Solid State Commun.* **83** (1992) 837.
13. R.A. Webb, S. Washburn, C.P. Umbach, and R.B. Leibowitz, *Phys. Rev. Lett.* **54** (1985) 2696.
14. G. Timp *et al.*, *Phys. Rev. Lett.* **58** (1987) 2814.
15. C.J.B. Ford *et al.*, *Phys. Rev.* **B43** (1991) 7339.